Raman spectrum of Pr_2CuO_4: Crystal-field transitions of Pr^{3+} and the A^* mode

M. L. Sanjuán and M. A. Laguna
Instituto de Ciencia de Materiales de Aragón, Universidad de Zaragoza-Consejo Superior de Investigaciones Científicas, Facultad de Ciencias, 50009 Zaragoza, Spain
(Received 2 March 1995)

We have investigated two aspects of the Raman spectrum of Pr_2CuO_4 and $(Pr,Ce)_2CuO_4$: crystal-field transitions within the Pr^{3+} levels and the appearance of a forbidden mode at 579 cm^{-1} in the zz spectrum, similar to the A^* mode observed in $R_{2-x}Ce_xCuO_4$ compounds for $x \neq 0$. In the region of intermultiplet $(^3H_4 \rightarrow {}^3H_5)$ transitions we observe two broad bands with Γ_1 symmetry centered at 2210 and 2685 cm^{-1}, that we attribute to transitions from the thermally populated first excited state (Γ_5) and from the ground state of Γ_3 symmetry, respectively. Other bands appearing between 450 and 650 cm^{-1} with the electric field in the x-y plane are attributed either to thermally activated crystal-field transitions or to in-plane oxygen vibrations. The appearance of the A^* mode in the undoped compound is ascribed to the presence of some degree of disorder in the oxygen sublattice. The model is similar to that explaining the A^* mode in Ce-doped samples, but the origin may be different; we suggest that in Pr_2CuO_4 it is due to the more expanded lattice compared, for instance, to that of Nd_2CuO_4, which results in lattice instability. Another possibility, relating the distortion to polaron self-trapping, is also discussed. The model is consistent with temperature-dependent measurements and also with the results in $(Pr,Ce)_2CuO_4$.

I. INTRODUCTION

The rare-earth cuprates of type R_2CuO_4 (R a lanthanide), parents of the so-called n-type superconductors $R_{2-x}Ce_xCuO_4$ ($x \approx 0.15$) crystallize in the tetragonal D_{4h}^{17} structure known as the T' phase. Though this symmetry is found in all x-ray diffractograms, there are numerous experimental results indicating that there is an intrinsic tendency to structural instability as the rare-earth radius is either reduced (from Eu to the right of the lanthanide series) or increased (to the left of Nd). In Ref. 1, we studied by means of Raman scattering the distortion of the CuO_2 planes in Gd_2CuO_4. A new, orthorhombic symmetry has recently been refined for Gd_2CuO_4.[2] At the beginning of the series, the more expanded compounds Pr_2CuO_4 and Nd_2CuO_4 do not present the Raman features indicating the type of distortion appearing in Gd_2CuO_4. However, Pr_2CuO_4 is at the limit of T' phase stability; the next compound with lighter R, La_2CuO_4, does not crystallize in the T' phase anymore but in the more compressed K_2NiF_4 or T phase, where the out-of-plane oxygens move to apical positions with respect to copper, resulting in octahedral instead of square-planar coordination for this atom.[3] Interstitial or apical oxygen atoms have also been reported in Nd_2CuO_4.[4] When doping Pr_2CuO_4 and Nd_2CuO_4 with bigger ions, such as La or Sr, smaller dopant concentrations are needed in the former to go from T' to T or T^* phases.[5,6] Stability conditions of the T' phase in terms of bond-length mismatch and ionic size are given in Ref. 6 and have been discussed in relation with electronic structure in Ref. 7.

Another type of distortion is present in Ce-doped compounds, which shows up in the activation of a strong forbidden mode with A_{1g} symmetry and frequency around 580 cm^{-1} (A^*) in the Raman spectrum of all doped compounds (and, strikingly, also in Pr_2CuO_4).[8–10] In Ref. 9 we assigned that mode to oxygen relaxation around the cerium impurity due to the smaller size and extra positive charge of Ce^{4+} with respect to the other R^{3+}, which would activate new Raman modes, in particular one (A^*) involving mostly the z vibration of oxygen atoms. To explain the appearance of the A^* model in Pr_2CuO_4 we proposed the existence of a small amount of Pr^{4+} ions, which would produce the same effect as a small cerium doping. In a subsequent paper, Billinge and Egami[11] studied by means of the neutron pair distribution function technique the disorder of the oxygen sublattice in $(NdCe)_2CuO_4$. Their results can be summarized as follows: There are two regions in this compound, one in which the CuO_2 planes are undistorted and another one where they are buckled, with oxygen shifts both in plane and along z axis. Corresponding displacements of the out-of-plane oxygen atoms were also found. This work suggested to us a new interpretation for the A^* mode in Pr_2CuO_4 that we present in this paper.

We also present new results on the subject of crystal-field (CF) levels of Pr^{3+} in Pr_2CuO_4 and $(PrCe)_2CuO_4$. There are several recent papers on inelastic neutron-scattering measurements of crystal-field excitations in the 0–340 meV region, covering the ground ($^3H_4$) (Refs. 12–14) and first excited ($^3H_5$) (Ref. 13) multiplets. Though the experimental results are coincident, there are some dispersion of fitted CF parameters, mainly due to the different approximations involved. A recent observation of electronic Raman transitions within the $^3H_4$ multiplet[15,16] seems to be in agreement with the energy level scheme predicted by the parameters obtained from neutron spectra. The authors of Ref. 15 failed to observe Raman transitions to the excited $^3H_5$ sublevels, some of which are observed in neutron scattering. We present here a Raman study of such transitions and new data on intra-$^3H_4$ transitions.

0163-1829/95/52(17)/13000(6)/$06.00

II. EXPERIMENTAL DETAILS

We have measured single crystals of $Pr_{2-x}Ce_xCuO_4$ ($x=0,0.18$) and Nd_2CuO_4. A Dilor XY spectrometer with intensified diode array detector was used with the $\lambda=514.5$ nm line of a Coherent Innova 200 argon laser as excitation source. The laser beam is focused on a few μm of the sample through the 50× objective of a microscope. Laser power was always kept at a few mW on the sample to avoid sample damage.

III. CF TRANSITIONS

In order to discuss on level symmetry and transition energies we summarize here the results of inelastic neutron scattering. Within the $^3H_4$ multiplet the spectrum of Pr_2CuO_4 consists at low temperature of two bands at 18 and $\approx$88 meV, the latter being comprised of at least two components.[12–14] The 18 meV band splits in $(PrCe)_2CuO_4$ (Refs. 13 and 17) showing a weak sideband at 14.5 meV. On rising the temperature a broad band with structure appears between 60 and 75 meV. In the 250–350 meV region, where transitions to the first excited multiplet are expected, a single broad band is observed, centered at 292 meV (2355 cm^{-1}), possibly containing several components.[13]

In spite of some dispersion of the fitted parameters, all three neutron works agree in the basic assumptions: the ground state of the $^3H_4$ multiplet split by the tetragonal crystal field (site symmetry of Pr^{3+} is C_{4v}) transforms as Γ_3 with respect to the crystal tetragonal axes.[18] The first excited state is a doublet (Γ_5) located at 18 meV, to which the first neutron transition occurs. The rest of the sublevels ($2\Gamma_1,\Gamma_2,\Gamma_4,\Gamma_5$) are gathered around 88 meV, the position of the Γ_4 and upper Γ_5 states being fixed by the neutron results, according to selection rules for dipolar magnetic transitions, which transform as Γ_2 and Γ_5 in C_{4v} symmetry. The detailed ordering varies from one work to another, the main difference being the position of the lowest Γ_1 state.

In the $^3H_5$ multiplet, with the same parameters, Boothroyd *et al.*[13] propose a pair of states around 295 meV, to explain the experimental band centered at 292 meV. Applying again the selection rules for neutron scattering, these states must have Γ_4 and Γ_5 symmetry. The rest of the $^3H_5$ sublevels lie at higher energies, up to 346 meV. We reproduce in Fig. 1 the level scheme of Boothroyd *et al.* for both multiplets, with indication of the neutron transitions observed both from the ground and first excited states. We also indicate Raman transitions observed within the $^3H_4$ multiplet and intermultiplet transitions of Γ_1 symmetry reported in this work.

In Fig. 2, we show the room-temperature (RT) zz Raman spectrum of Pr_2CuO_4 and $Pr_{1.82}Ce_{0.18}CuO_4$ single crystals in the region of $^3H_4\rightarrow{}^3H_5$ transitions. Three bands are observed: A narrow peak at 2327 cm^{-1}, due to scattering from N_2 molecules, and two broad bands, one at 2210 cm^{-1} (A), also observed weakly in $z(xx)z$ configuration, and another one at 2685 and 2700 cm^{-1} (B) in the pure and doped compounds, respectively. No other peaks are found in zz from 1700 to 2800 cm^{-1}. The fact that the same zz spectrum is observed in $(PrCe)_2CuO_4$ and not in related compounds of other rare earths and the region where the bands appear suggest that the A and B bands are intermultiplet CF transitions of Pr^{3+}. At 10 K, band B is split into two components at 2616 ($B1$) and 2699 ($B2$) cm^{-1} (see Fig. 3).

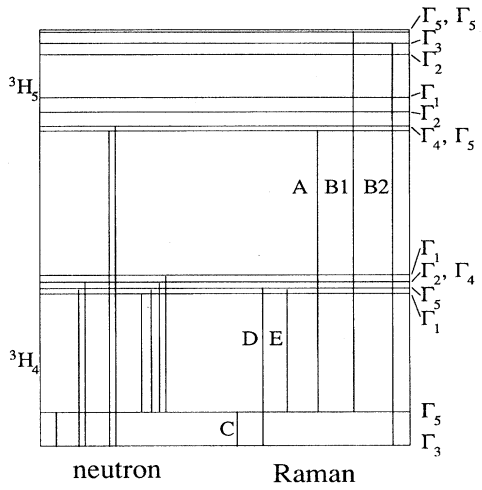

FIG. 1. Level scheme of $^3H_4$ and $^3H_5$ multiplets of Pr^{3+} in Pr_2CuO_4 (C_{4v} symmetry) according to the parameters of Ref. 11. Some transitions observed in neutron (Ref. 11) and Raman scattering (Ref. 13 and this work) are indicated. Labels A, $B1$, and $B2$ indicate intermultiplet CF transitions observed in zz spectra; C and D are intramultiplet transitions of Γ_5 symmetry reported in Ref. 13 and in this work, and E indicates the $\Gamma_5\rightarrow\Gamma_5$ transition that contributes to the spectra of Fig. 4(a), as well as to the sideband of the A^* mode (Fig. 6).

Bands A and B can be interpreted within the energy level diagram of Fig. 1. In C_{4v} symmetry, Raman-active transitions transform as Γ_1, Γ_3, Γ_4, and Γ_5 representations, and the activity of each level can be found from the multiplication rules (assuming a Γ_3 ground state) $\Gamma_3\times\Gamma_1=\Gamma_3$, $\Gamma_3\times\Gamma_2=\Gamma_4$, $\Gamma_3\times\Gamma_3=\Gamma_1$, $\Gamma_3\times\Gamma_4=\Gamma_2$ (inactive), and

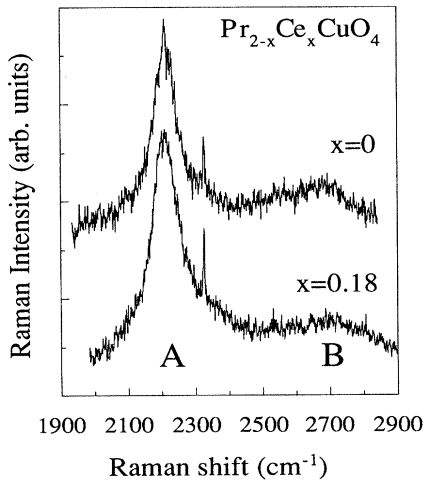

FIG. 2. RT zz spectrum of pure ($x=0$) and doped ($x=0.18$) Pr compounds, showing intermultiplet transitions of Γ_1 symmetry. The peak at 2327 cm^{-1} is due to N_2 scattering.

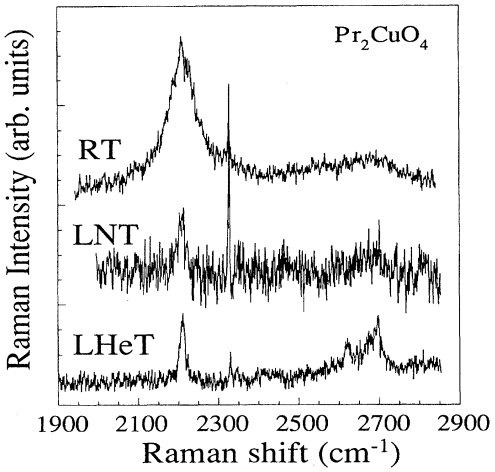

FIG. 3. Temperature evolution of the intermultiplet transitions of Fig. 2.

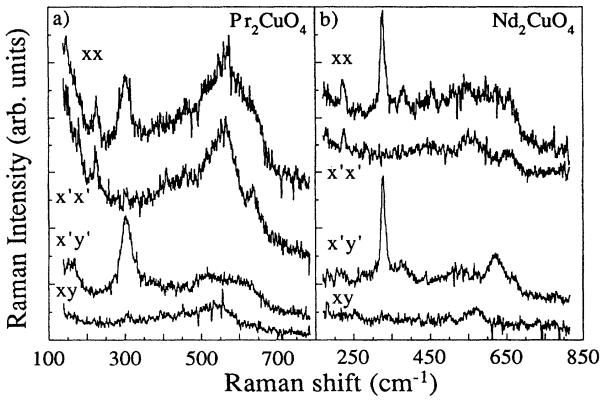

FIG. 4. RT in-plane spectra of Pr_2CuO_4 and Nd_2CuO_4 with indication of incident and scattered electric field. The spectra show, besides the allowed A_{1g} and B_{1g} phonons, broad features in the 400–700 cm^{-1} region, discussed in the text.

$\Gamma_3\times\Gamma_5=\Gamma_5$. With a Γ_3 ground state, only one Γ_1 Raman transition is expected to the $^3H_5$ multiplet, since there is just one Γ_3 state in this multiplet. From Ref. 13 we find that this transition would occur at an energy close to 2700 cm^{-1}, where band $B2$ is found. Then we assign band $B2$ to the $\Gamma_3(^3H_4)\rightarrow\Gamma_3(^3H_5)$ intermultiplet transition. Since no other Γ_1 bands are expected in this energy region, bands A and $B1$ must be due to transitions thermally excited from the $\Gamma_5(^3H_4)$ doublet at 18 meV (we see it at 156 cm^{-1} at 10 K). Γ_1 transitions are active between pairs of Γ_5 states ($\Gamma_5\times\Gamma_5=\Gamma_1+\Gamma_2+\Gamma_3+\Gamma_4$) and are thus expected, with the calculations of Ref. 13, at 2237, 2632, and 2644 cm^{-1} in the region of intermultiplet transitions at low temperature. Then we assign band A [2212 cm^{-1} at liquid-helium temperature (LHeT)] to the transition from the thermally populated Γ_5 state at 156 cm^{-1} to the first Γ_5 doublet of the $^3H_5$ multiplet, whose position is thus determined as $\approx$2368 cm^{-1}, very close to the mean frequency found for the intermultiplet neutron transition in Ref. 13, and band $B1$ (2616 cm^{-1} at LHeT) to the transition to the second Γ_5 state, placed in this way at 2772 cm^{-1}. This attribution is corroborated by the temperature evolution of the zz spectrum, shown in Fig. 3. At LHeT bands A and $B2$ are about 20 cm^{-1} wide and have nearly the same intensity. As temperature is raised both bands broaden considerably and the A band intensity increases relative to that of the B band. Band $B1$ is broadened and lost beyond detection under band $B2$. We note that the RT spectrum has been measured with a different set up, so that the absolute intensities may not be significative, though we have tried to rescale the spectra by means of the A_{1g} phonon intensity. The fact that bands A and $B1$ are seen at the lowest temperatures indicates that the sample temperature is much higher than the nominal value. Increments as high as 60 K must occur in order to populate the Γ_5 excited state appreciably. This is due to the use of microscope and to the bad thermal conductivity of the sample.

We turn now to Raman transitions within the $^3H_4$ multiplet. In Ref. 15 peaks are found, at 20 K, at 156 and 685 cm^{-1} (our values are 156 and 701 cm^{-1}, respectively) in the xz spectrum (Γ_5 symmetry), and another one at $\approx$540 cm^{-1} above 100 K in zz and xz, that the authors attribute to thermally excited transitions between two Γ_5 doublets. They also find a weak future in the xx spectrum, at the same frequency as the highest Γ_5 peak, that they assign to a Γ_3 transition ($\Gamma_4\rightarrow\Gamma_2\Rightarrow\Gamma_3$; these authors follow the labeling of Allenspach *et al.*[12] for the ground state as Γ_4). In this scheme, the Γ_2 state lies at 664 cm^{-1} (rather far, in any case, from the observed frequency). However, we note again that in Ref. 12 axes are rotated at 45° with respect to the tetragonal lattice; therefore, that transition should not be observed at a Γ_3 if measurements are performed along tetragonal axes, as is the case, but as a Γ_4, observable in the xy configuration. Then, the observation of the 685-cm^{-1} feature in xx must be a polarization leakage, as there are others in Ref. 15 due to imperfect sample orientation. The detection of the thermally excited 540 band in xz, as well as that of the A^* phonon, is also probably due to a leakage, since $\Gamma_5\times\Gamma_5$ does not contain Γ_5 and the A^* phonon has perfect A_{1g} symmetry.

We have performed measurements in the low-frequency region with the electric field both in and perpendicular to the x-y plane, as a function of temperature, with the aim of detecting other allowed CF transitions. The RT spectra for the configurations $z(xx)z$, $z(xy)z$, $z(x'x')z$, and $z(x'y')z$ (x' and y' at 45° from x,y) are shown in Fig. 4(a). The most prominent feature is the broad band centered near 550 cm^{-1} with mostly Γ_1 character, though it is also present in Γ_3 ($x'y'$) and Γ_4 (xy) spectra with weaker intensity. Other components with frequency $\geq$600 cm^{-1} are seen in Γ_1 and Γ_3 spectra.

There are two possible explanations for this spectrum: CF transitions and phonons. From Fig. 1 we see that no transitions from the ground state are expected between 150 and 650 cm^{-1}. Transitions from the thermally populated Γ_5 state have been reported in the neutron spectrum at 150 K in Ref. 13. Peaks are found in the 60–75 meV region (roughly 480–600 cm^{-1}) involving transitions from Γ_5 to the upper Γ_1, Γ_5, Γ_4, Γ_2, and Γ_1 levels. From these, only the $\Gamma_5\times\Gamma_5$ transition is allowed in Raman scattering with in-plane electric field. Since $\Gamma_5\times\Gamma_5=\Gamma_1+\Gamma_2+\Gamma_3+\Gamma_4$ (Γ_2 inactive), the transition is allowed in xx, xy, $x'x'$, $x'y'$ (and zz), and

is expected, according to our values for the position of both Γ_5 levels, at 545 cm^{-1}. Thus it can explain (or contribute partially to) the large band centered at 550 cm^{-1}. A Γ_3 transition from the Γ_3 ground state to the first Γ_1 level is expected around 600 cm^{-1}. Then, it can partially give account of the high-frequency side of the xx and $x'y'$ spectra. However, the CF spectrum is probably superposed in all polarizations with peaks of phononic origin, either simple or double. We present in Fig. 4(b) the in-plane spectra of Nd_2CuO_4, which look quite similar to those of Pr_2CuO_4. Raman peaks in the 400–700 cm^{-1} region have been attributed either to single-phonon modes (for Pr_2CuO_4, Ref. 10) or to double phonons (for Nd_2CuO_4, Ref. 19). Since all the Raman-active single phonons have already been identified, in the former case some lattice disorder (oxygen vacancies, for instance) is needed in order to activate forbidden modes. We note that low-temperature neutron spectra of Pr_2CuO_4 and $(Pr,Ce)_2CuO_4$ reported in Ref. 20 present low-intensity peaks in the 30–75 meV region that the authors assign to single phonons. Specifically, a broad band centered at 550 cm^{-1} in the Pr_2CuO_4 neutron spectrum of Ref. 20 is coincident with the main band of our spectra shown in Fig. 4. Then we conclude that both thermally activated CF transitions and phonon modes can be present in our in-plane spectra. Low-temperature measurements have not been very useful in clarifying the origin of the bands, since even at nominal LHeT heating is enough to populate the Γ_5 electronic state, so that both types of peaks can be expected. However, the broad in-plane spectrum shows a remarkably different behavior compared to the intermultiplet CF transitions of Fig. 3: while the latter narrow at low temperature to a few cm^{-1}, the former show an almost temperature-independent width, thus supporting the phononic rather than the CF origin. We also note that the broadening of CF transitions with increasing temperature, also reported in Ref. 15, seems to be specific to Pr compounds: the linewidth of Nd^{3+} CF peaks in Nd_2CuO_4 (Ref. 19) increases only from 10 to 14 cm^{-1} on heating from 10 to 300 K, while bands of our Fig. 2 are nearly 100 cm^{-1} wide.

In order to better characterize the thermally excited transition reported at 540 cm^{-1} in Ref. 15 as well as the A^* and A_{1g} phonons, we have followed them as a function of temperature. We do not observe any of these peaks in the xz configuration, which is in agreement with the symmetry of the phonons and of the CF transition. Figure 5 shows the RT zz and xz spectrum of the pure and Ce-doped Pr compounds and the xz spectrum of Pr_2CuO_4 at LHeT. The peaks seen at 126 and 124 cm^{-1} in the RT xz spectra of Pr_2CuO_4 and $(Pr,Ce)_2CuO_4$, respectively, are attributed to the rare-earth E_g mode. (In Ref. 21 a value of 128 cm^{-1} is given for Pr_2CuO_4.) The appearance of weak A_{1g} and A^* modes in the low-temperature xz spectrum is due to the lack of exit polarizer in that particular experiment. The region of the A^* mode is shown in Fig. 6 for several temperatures and the data for A_{1g} and A^* modes are collected in Fig. 7.

The frequency softening with increasing temperature of the A^* and A_{1g} phonons is similar to that found for the same modes in $(NdCe)_2CuO_4$. The most peculiar feature is the splitting of the A^* band seen in Fig. 6 at temperatures as low as 40 or 50 K. A weak component appears at 553 cm^{-1}

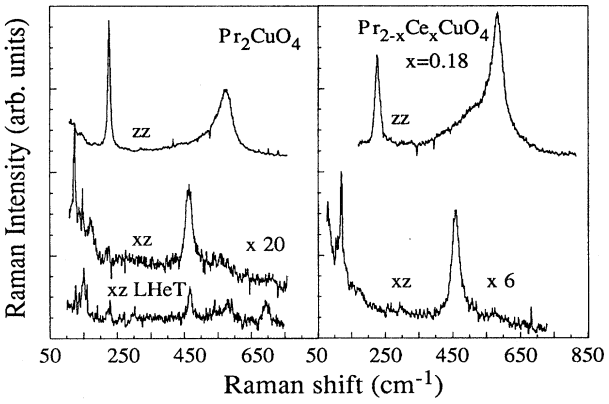

FIG. 5. RT zz and xz spectra of pure and doped Pr compounds showing the A_{1g}, A^*, and $2E_g$ modes. A feature appearing close to 170 cm^{-1} has not been interpreted yet. In the left part of the figure we also show the xz spectrum of Pr_2CuO_4 measured at LHeT.

already at the lowest temperatures, then softens down to 548 cm^{-1} around 100 K and finally shifts again toward higher frequencies up to 560 cm^{-1}. These frequencies were obtained from a fit with two Lorentzians and a linear baseline. The intensity of the low-frequency sideband increases with temperature, and also with respect to that of the main A^* peak. For the lowest temperatures, two close Lorentzians were needed in the region 575–590 cm^{-1}, besides the low-frequency sideband. The evolution from 130 to 300 K,with the increase of a peak at a frequency lower than the A^*, is coincident with the results of Ref. 15 and agrees with a thermally activated $\Gamma_5 \rightarrow \Gamma_5$ CF transition [the same that contributes to the 550 cm^{-1} band of Fig. 4(a)]. However, we have no explanation for the remarked frequency shift and also for the low-T behavior. No other intramulitplet CF transition of Γ_1 symmetry is allowed; it might be another disorder-activated vibration, but is peculiar temperature dependence is to be explained.

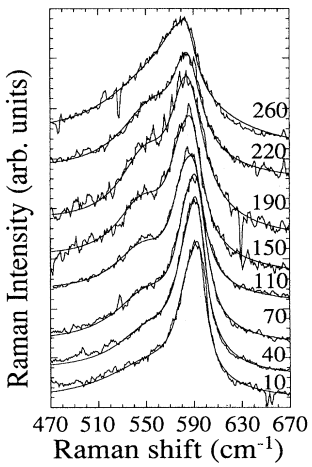

FIG. 6. Temperature evolution of the A^* mode and adjacent peak. The spectra are taken in zz polarization.

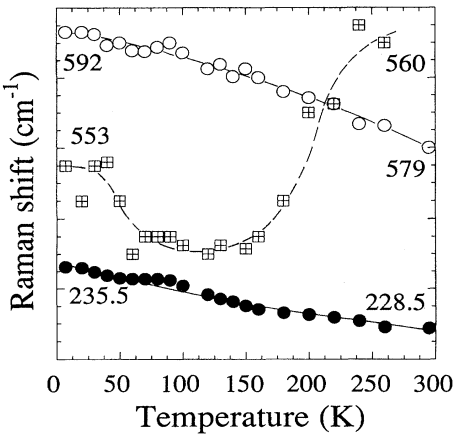

FIG. 7. Temperature evolution of Raman frequency of the A_{1g} phonon (●), A^* phonon (○), and left sideband of A^* (⊞).

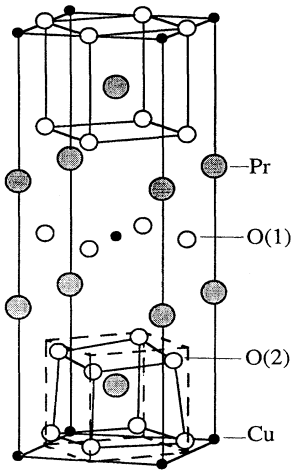

FIG. 8. T'-phase unit cell showing some disorder in the oxygen sublattice and how it affects the Pr environment.

IV. ORIGIN OF THE A^* MODE

Resuming here the preceding discussion of lattice distortion in this family of cuprates, we suggest that there may be in Pr_2CuO_4 slight distortions from perfect oxygen ordering, perhaps as a consequence of the lattice being expanded near the stability limit of a T' phase. The displacement of oxygen atoms allows the appearance of the A^* mode (and perhaps other vibrations) in undoped Pr_2CuO_4. Cerium doping, expanding the CuO_2 plane and producing an inward relaxation of oxygens toward Ce^{4+}, would favor the distortion, thus explaining the increase of the A^* band in $(PrCe)_2CuO_4$ with respect to Pr_2CuO_4 (Fig. 5). There is another point in favor of the existence of oxygen sublattice disorder: The allowed modes due to O(2) vibrations are much wider in Pr_2CuO_4 than in Nd_2CuO_4. The B_{1g} mode seen in Fig. 4, for instance, is four times wider in the Pr compound. The relation is close to 2 for the oxygen E_g mode. In contrast, the rare-earth A_{1g} and E_g modes have the same width in the Pr and Nd pure compounds.

We would like now to discuss the origin of the oxygen sublattice disorder in Pr_2CuO_4 and in cerium-doped samples. As we have said in the Introduction, in their paper on $(NdCe)_2CuO_4$ (Ref. 11) Billinge and Egami propose the coexistence of distorted and undistorted regions in the sample, with oxygen shifts of the order of 0.1 Å in the distorted regions. They state that the buckling of CuO_2 planes is not an intrinsic feature of T' structure based on ion size mismatch and propose that the distortion is rather due to polaron formation by hole self-trapping in narrow oxygen bands close to the Fermi level. The average size of distorted regions (about 6 Å) would be a measure of the spatial extent of the polaron wave function. It is not clear in their work which is the role played by cerium (electron) doping in the appearance of such polarons. Though we have no cerium in Pr_2CuO_4, the presence of the A^* mode with similar characteristics as in doped compounds (except for its resonant behavior, see Ref. 9) suggests that they have a common origin. We sketch in Fig. 8 the T' unit cell with some disorder in the oxygen sublattice (lower part of the figure), compared to the undistorted structure (upper part). Our data are not precise enough to determine the exact positions of the oxygen atoms in the distorted areas, so that we propose a random, rather than ordered, oxygen displacement. This last possibility would lead to new activated Raman modes. But taking into account the reduced extension of distorted regions, these would be more like local modes, such as the A^* mode, rather than phonons, and perhaps of too weak intensity to be detected. We have proposed the instability of the lattice as the most simple mechanism, but it is indeed striking that it leads to the same A^* activation as cerium doping. Another possibility is to assume that holes are also being self-trapped in oxygens close to Pr^{3+}. This would result in short-range disorder in the Pr environment and would allow the activation of the A^* mode. We note that, recently, Booth *et al.*[22] have proposed the existence of either some Pr^{4+} or Pr^{3+} $(4f^2\underline{L})$-O, with a hole localized in a nearest-neighbor oxygen, to explain the appearance of two types of Pr-O bonds in the x-ray-absorption fine-structure spectra of $Y_{1-x}Pr_xBa_2Cu_3O_7$. The presence of different types of Pr environments has been proposed to explain the width and even splitting of the neutron peaks in $(PrCe)_2CuO_4$ (Refs. 13 and 17) and $(NdCe)_2CuO_4$ (Ref. 23). The question arises as to what Raman spectrum can be expected if there are in fact two (or more) Pr sites in the doped compound. No splitting or significative broadening of the intermultiplet CF transitions in $(Pr,Ce)_2CuO_4$ is found in Fig. 2 at RT. There are different possible explanations for this absence: it might be that one of the sites occurs with much lower probability than the other, or that it is so distorted that the transition is broadened beyond detection, and so on. We neither observe any substantial difference between the RT spectra of pure and doped compounds in the region of intra-$^3H_4$ multiplet (see Fig. 5). However, we note that in Ref. 16 the authors report on an asymmetric broadening of the 150-cm^{-1} CF band that they attribute to the existence of different Pr sites.

Summing up our work, we present Raman spectra showing CF transitions to the first excited multiplet of Pr^{3+} in pure and doped Pr_2CuO_4. Spectra in the region of phonon modes and of CF transitions within the ground-state multiplet are also given. We propose an interpretation for the A^*

mode as a disorder-activated mode, as a consequence of Pr_2CuO_4 being close to the limit of T' phase stability, and discuss the connection with other results and models appeared in the literature, proposing the existence of some Pr^{4+} or Pr^{3+} + ligand hole. Ce doping induces that type of distortion in all R_2CuO_4 compounds, and increases the preexisting disorder in Pr_2CuO_4.

ACKNOWLEDGMENTS

We thank Dr. P. C. Canfield and Dr. Z. Fisk, from Los Alamos National Laboratory (New Mexico), and Dr. S. Piñol, from the Instituto de Ciencia de Materiales de Barcelona (Barcelona, Spain) for providing us with the Pr_2CuO_4 and $(PrCe)_2CuO_4$ samples, respectively, used in this work.

[1] M. A. Laguna, M. L. Sanjuán, A. Butera, M. Tovar, Z. Fisk, and P. Canfield, Phys. Rev. B **48**, 7565 (1993).

[2] M. Braden, W. Paulus, A. Cousson, P. Vigoureux, G. Heger, A. Gourkassov, P. Bourges, and D. Petitgrand, Europhys. Lett. **25**, 625 (1994).

[3] Actually, the RT structure of La_2CuO_4 is orthorhombic ($D_{2h}{}^{18}$). The T phase is achieved above 432 K.

[4] P. Ghigna, G. Spinolo, A. Filipponi, A. V. Chadwick, and P. Hanmer, Physica C **246**, 345 (1995); P. G. Radaelli, J. D. Jorgensen, A. J. Schultz, J. L. Peng, and R. L. Greene, Phys. Rev. B **49**, 15 322 (1994).

[5] H. Y. Hwang, S.-W. Cheong, A. S. Cooper, L. W. Rupp, B. Batlogg, G. H. Kwei, and Z. Tan, Physica C **192**, 362 (1992); K. K. Singh, P. Ganguly, and C. N. R. Rao, Mater. Res. Bull. **17**, 493 (1982).

[6] M. J. Rosseinsky, K. Prassides, and P. Day, Physica C **161**, 21 (1989); Y. Y. Xue, P. H. Hor, R. L. Meng, Y. K. Tao, Y. Y. Sun, Z. J. Huang, L. Gao, and C. W. Chu, *ibid.* **165**, 357 (1990).

[7] J. B. Goodenough and A. Manthiram, J. Solid State Chem. **88**, 115 (1990); Y. T. Zhu and A. Manthiram, Phys. Rev. B **49**, 6293 (1994).

[8] E. T. Heyen, R. Liu, M. Cardona, S. Piñol, R. J. Melville, D. McK. Paul, E. Morán, and M. A. Alario-Franco, Phys. Rev. B **43**, 2857 (1991).

[9] M. L. Sanjuán, M. A. Laguna, S. Piñol, P. Canfield, and Z. Fisk, Phys. Rev. B **46**, 8683 (1992).

[10] S. Sugai, T. Kobayashi, and J. Akimitsu, Phys. Rev. B **40**, 2686 (1989).

[11] S. J. L. Billinge and T. Egami, Phys. Rev. B **47**, 14 386 (1993).

[12] P. Allenspach, A. Furrer, R. Osborn, and A. D. Taylor, Z. Phys. B **85**, 301 (1991).

[13] A. T. Boothroyd, S. M. Doyle, D. McK. Paul, and R. Osborn, Phys. Rev. B **45**, 10 075 (1992).

[14] C.-K. Loong and L. Soderholm, Phys. Rev. B **48**, 14 001 (1993).

[15] J. A. Sanjurjo, C. Rettori, S. Oseroff, and Z. Fisk, Phys. Rev. B **49**, 4391 (1994).

[16] J. A. Sanjurjo, G. B. Martins, P. G. Pagliuso, E. Granado, I. Torriani, C. Rettori, S. Oseroff, and Z. Fisk, Phys. Rev. B **51**, 1185 (1995).

[17] W. Henggeler, G. Cuntze, M. Klauda, J. Mesot, A. Furrer, and G. Saemann-Ischenko, Physica C **235-240**, 1697 (1994).

[18] There seems to be some confusion about the symmetry of the ground state that derives from the election of axes either along the tetragonal ones or along those of the pseudocube of oxygens around Pr, which are rotated 45° with respect to the former. This results in interchanging Γ_4 and Γ_3 representations. In the first case, as in Ref. 12, the ground state transforms as a Γ_3. In Ref. 10, though the parameter signs correspond to tetragonal axes, the level labeling of their Fig. 4(b) corresponds to cubic axes, so that the ground state transforms as Γ_4.

[19] S. Jandl, M. Iliev, C. Thomsen, T. Ruf, M. Cardona, B. M. Wanklyn, and C. Chen, Solid State Commun. **87**, 609 (1993).

[20] I. W. Sumarlin, J. W. Lynn, D. A. Neumann, J. J. Rush, C-K. Loong, J. L. Peng, and Z. Y. Li, Phys. Rev. B **48**, 473 (1993).

[21] D. M. Mateev, V. N. Popov, V. G. Hadjiev, and M. N. Iliev, Physica C **235-240**, 1189 (1994).

[22] C. H. Booth, F. Bridges, J. B. Joyce, T. Claeson, Z. X. Zhao, and P. Cervantes, Phys. Rev. B **49**, 3432 (1994).

[23] A. Furrer, P. Allenspach, J. Mesot, and U. Staub, Physica C **168**, 609 (1990).

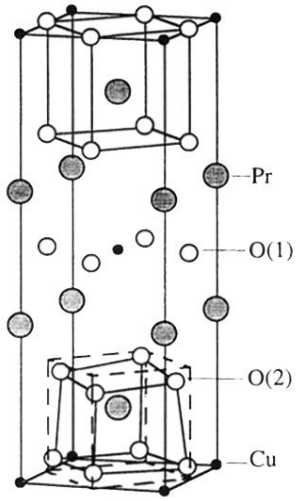

FIG. 8. T'-phase unit cell showing some disorder in the oxygen sublattice and how it affects the Pr environment.